

The emission mechanism in magnetically dominated GRB outflows

Paz Beniamini^{1a} & Tsvi Piran^{1b}

(a) paz.beniamini@mail.huji.ac.il; (b) tsvi.piran@mail.huji.ac.il

ABSTRACT

We consider the conditions within Gamma-Ray Burst (GRB) emission region that is Poynting flux dominated. Due to the enormous magnetic energy density, relativistic electrons will cool in such a region extremely rapidly via synchrotron. As there is no known mechanism that can compete with synchrotron it must be the source of the prompt sub-MeV emission. This sets strong limits on the size and Lorentz factor of the outflow. Furthermore, synchrotron cooling is too efficient. It overproduces optical and X-ray as compared with the observations. This overproduction of low energy emission can be avoided if the electrons are re-accelerated many times ($\gtrsim 5 \times 10^4$) during each pulse (or are continuously heated) or if they escape the emitting region before cooling down. We explore the limitations of both models, practically ruling out the later and demonstrating that the former requires two different acceleration mechanisms as well as an extremely large magnetic energy to Baryonic energy ratio. To be viable, any GRB model based on an emission region that is Poynting flux dominated must demonstrate how these conditions are met. It is more likely that jets that are launched as magnetically dominated dissipate somehow most of their magnetic energy before the emission region.

1. Introduction

It is generally accepted that Gamma Ray Bursts (GRBs) are powered by ultra relativistic jets (with a Lorentz factor $\Gamma \geq 100$) carrying large isotropic equivalent luminosities ($L_{iso} \approx 10^{53}$ erg/sec) which are dissipated at large distances ($r \approx 10^{13} - 10^{17}$ cm) from the central engine. A major puzzle concerning these jets involves their composition. The two leading alternatives are either baryonic fireballs (Shemi & Piran 1990) or magnetically (Poynting flux) dominated jets (Usov 1992; Thompson 1994; Mészáros et al. 1997; Lyutikov & Blandford 2003). The thermal pressure at the base of a blazar jet is insufficient to support a baryonic outflow and therefore, blazars' jets must be magnetically dominated. The situation for GRBs is less certain as with

¹Racah Institute for Physics, The Hebrew University, Jerusalem, 91904, Israel

smaller size engines the thermal pressure in the base could be sufficient to drive baryonic outflows. However, modeling of some GRBs' engines based on accretion disks suggest that the Poynting flux jet power is much stronger than the thermal driven outflow that derived from neutrino annihilation Kawanaka, Piran, & Krolik (2013). Furthermore, the fact that blazars jets are magnetically driven, suggests that this might also be the case for GRBs.

Another major puzzle concerning GRBs is the nature of the radiation mechanism that produces the prompt emission. The non thermal spectrum has led to the suggestion that the prompt emission is produced by synchrotron mechanism (Katz 1994; Rees and Mészáros 1994; Sari et al. 1996, 1998). This was supported by the reasonable association of the afterglow emission with synchrotron radiation. However, observations of many bursts showing lower energy spectral slopes steeper than the “synchrotron line of death” (Crider et al. 1997; Preece et al. 1998, 2002) have led to the suggestion that the prompt emission must be produced by another mechanism.

Recently, detailed analysis of prompt spectra has shed some new light on this debate. First, there have been several cases, e.g. GRB 080916C, in which there is a strong upper limit on the thermal component (Zhang et al. 2009), or GRBs: 100724B, 110721A, 120323A, where a thermal component was possibly detected but with only a small fraction (5 – 10%) of the total energy in the thermal component (Guiriec et al. 2011, 2013; Axelsson et al. 2012). Second, refined time dependent spectral analysis in several bright bursts (Guiriec 2012) has suggested that GRB spectra may be better fitted with a multi component model instead of the classical “Band function”. In the multi component model, the spectrum is composed of a superposition of a Band function peaking at few hundred keV and carrying most of the energy, a black body component at a few tens of keV with 5 – 10% of the energy and in some cases an additional power law component extending up to a few hundred MeV and carrying up to 40% of the total energy. In these fits, the lower energy spectral slope of the Band function becomes softer compared with the Band only fits, and is consistent with slow cooling synchrotron (i.e. the synchrotron “line of death” problem is removed). The direct detection of a weak photospheric component in those GRBs, suggests that the “thermal signature” is sub-dominant and it is not the main radiation source in operation during the prompt. To sum, these later results support synchrotron emission as the main radiation mechanism while requiring additional mechanisms to produce the other components.

In this paper, we show that the two fundamental questions presented above, regarding the composition of GRB jets and main radiation mechanism are strongly interconnected. We explore Poynting flux dominated emission regions. As relativistic electrons are essential to produce the observed prompt emission (regardless of the specific emission mechanism) then due to the high magnetic energy density, a significant synchrotron signal (not necessarily in the sub-MeV band) must be produced as well. We compare the expected synchrotron fluxes with upper limits on prompt observations at the optical, X-ray and GeV bands, and show that in order for the synchrotron flux to be consistent with observations, the gamma-ray process should be unrealistically

efficient. Thus, in a magnetically dominated emission region, synchrotron emission must be the main emission mechanism during the prompt phase. This sets numerous limits on the conditions, such as the radius and Lorentz factor of the emitting regions.

Additionally, as the synchrotron is extremely efficient, the electrons will cool rapidly and in addition to producing a $\nu^{-1/2}$ low energy spectral slope they will over produce optical and X-ray. This is inconsistent with observational limits within these energy bands. Thus, this low energy fast cooling tail must be avoided. We show that this inconsistency may be alleviated if electrons are re-accelerated many times during a single pulse or if they escape from the emitting region before they cool down. We examine the limitations and conditions in which either one of these mechanisms can operate.

This paper is organized as follows. In §2 we discuss the basic concepts and the parameter phase space of the model. In §3 we discuss the general characteristics of synchrotron emission, focusing on the typical frequencies and the cooling timescale. In §4, we find the constraints on the parameter space from observed limits on the flux in different bands. We discuss the implications of the results on the synchrotron emission mechanism in §5 and we conclude and summarize in §6.

2. General Considerations

We consider the situation in which the main sub-MeV peak of the prompt GRB emission is produced within a magnetically dominated flow by some unknown radiation mechanism. Due to the large magnetic energy density, a significant synchrotron signal (not necessarily in the sub-MeV) is expected. We explore this “synchrotron signature” and compare it with observational limits in various energy bands.

The emitting region associated with the production of a single pulse can be described by 6 parameters (see Beniamini & Piran (2013)). These can be chosen as: the co-moving magnetic field strength, B' , the number of relativistic emitters, N_e , the ratio of magnetic to electrons' energy in the jet, ϵ , the bulk Lorentz factor of the source with respect to the GRB host galaxy, Γ , the typical electrons' Lorentz factor in the source frame, γ_m , and the ratio between the shell crossing time and the angular timescale, k . The primes denote quantities in the co-moving frame whereas un-primed quantities reflect quantities measured in the lab frame. In principle, a full description should also list θ , the jet opening angle. However, the source can be treated as spherically symmetric as long as $\Gamma^{-1} < \theta$ which holds during the prompt phase, where $\Gamma \geq 100$. We therefore do not solve for θ and use isotropic equivalent quantities throughout the paper.

An upper limit on the emitting radius is given by the variability time scale, $t_p \geq t_{ang} \equiv$

$R/(2c\Gamma^2)$. We define a dimensionless parameter k such that $kR/2\Gamma^2$ is the shell's width:

$$t_{cross} \equiv \frac{kR}{2c\Gamma^2} = kt_{ang}. \quad (1)$$

With this definition, the pulse duration is:

$$t_p \equiv \frac{(k+1)R}{2c\Gamma^2}. \quad (2)$$

Clearly, for $k \leq 1$ the pulse width is determined by angular spreading.

The relativistic electrons are assumed to have a power-law distribution of Lorentz factors:

$$\frac{dN_e}{d\gamma} = C\left(\frac{\gamma}{\gamma_m}\right)^{-p}, \quad (3)$$

(where C is a normalization constant) which holds for $\gamma_m < \gamma < \gamma_{Max}$. The typical Lorentz factor of the electrons, γ_m is determined by the total internal energy of the electrons:

$$E'_e = \frac{p-1}{p-2} \gamma_m N_e m_e c^2 \equiv \epsilon_e E'_{tot}, \quad (4)$$

where N_e is the number of relativistic electrons, E'_{tot} is the energy of the flow in the co-moving frame and the ratio of the total energy in the relativistic electrons to the total internal energy is denoted by ϵ_e . It is important to stress that in case the synchrotron cooling time is shorter than the dynamical time, ϵ_e does not reflect the instantaneous energy ratio of the relativistic electrons to the total energy, which could be much smaller. Furthermore, for models invoking re-acceleration or continuous heating (that are further discussed in §5), Eq. 4 should be multiplied by the number of acceleration processes. We expect the power-law index p to be of the order $p \sim 2.5$ (Achterberg et al. 2001; Bednarz et al. 1998; Gallant & Achterberg 1999). Indeed this value agrees with observations of both the GRB prompt and afterglow phases (Sari and Piran 1997; Panaitescu and Kumar 2001). If γ_{Max} arises due to Synchrotron losses at the energy where the acceleration time equals to the energy loss time (de Jager 1996) then:

$$\gamma_{Max} = 4 \times 10^7 f B'^{-1/2}, \quad (5)$$

where f is a numerical constant of order unity which encompasses the details of the acceleration process and B' is the co-moving magnetic field. In a shock-acceleration scenario this depends on the amount of time the particle spends in the downstream and upstream regions (Piran & Nakar 2010; Barniol Duran & Kumar 2011).

In a single zone model the magnetic field is assumed to be constant over the entire emitting region (we explore deviations from this assumption in §5). The magnetic energy is:

$$E'_B = \frac{B'^2}{8\pi} 4\pi R^2 \frac{kR}{\Gamma} \equiv \epsilon_B E'_{tot}, \quad (6)$$

where kR/Γ is the thickness of the shell in the co-moving frame and ϵ_B is the fraction of magnetic to total energy. By definition in a magnetic dominated outflow (that we consider here) $\epsilon_B \approx 1$.

We define ϵ_γ as the efficiency of conversion between total and (isotropic equivalent) radiated energy in gamma rays. The energy of the observed sub-MeV flux, is huge and already highly constraining astrophysical models. In addition, observations of afterglows, show that the energy released in the afterglow is at most that of the prompt (Panaitescu and Kumar 2002; Granot et al. 2006; Fan et al. 2006). The implication is that a significant amount of the kinetic energy is released in the prompt phase and the efficiency of the gamma ray process should be high. Here we choose a canonical value of $\epsilon_\gamma = 0.1$. Assuming that the gamma ray emission arises from relativistic electrons, the efficiency is limited by the amount of energy that passes at some point through the electrons: $\epsilon_\gamma < \epsilon_e$. The requirement $\epsilon_\gamma = 0.1$ leads to $\epsilon_e > 0.1$. The narrow range of ϵ_e , together with the fact that most relevant parameters depend only weakly on its value, mean that in exploring the parameter space it is possible to assume a constant $\epsilon_e = 0.1$ with no loss of generality.

Γ is highly constrained by the opacity to photon-photon pair production (Fenimore et al. 1993; Piran 1995; Woods 1995; Sari & Piran 1999; Lithwick & Sari 2001; Nakar et al. 2005; Zou & Piran 2010) to within the range: $50 \leq \Gamma \leq 3000$. Here we choose, for illustrative purposes, three canonical values: $\Gamma = 50, 300$ and 1000 .

Two main observations define the relevant parameters of the prompt emission process. The duration of a typical pulse and its isotropic equivalent energy. Again for illustrative purposes we take fiducial values. We consider a typical pulse with an isotropic equivalent energy of $E_{tot} = 5 \times 10^{52}$ erg, and a duration, $t_p = 0.5$ sec (both in the host frame). This reduces the number of free parameters from six to two, which we choose as: (γ_m, R) . Six further constraints described in §4 further limit the allowed region within this parameter space.

3. The synchrotron signature

The synchrotron emission is characterized by two frequencies. ν_m , the synchrotron frequency for the typical energy electron, and the cooling frequency, ν_c , the frequency at which electrons cool via synchrotron¹, on the pulse time-scale. The former frequency is given by:

$$\nu_m = \Gamma \gamma_m^2 \frac{q_e B'}{2\pi m_e c}. \quad (7)$$

¹For magnetically-dominated jets, one may easily ignore losses by IC, so long as the electrons are at least mildly relativistic

The later satisfies:

$$\nu_c = \frac{18\pi q_e m_e c}{\sigma_T^2 B^3 \Gamma t_a^2}, \quad (8)$$

where t_a the dynamical time (for which $t_a = t_p$) or the time available for cooling between two consecutive acceleration episodes (Kumar & McMahon 2008) whichever is shorter. The synchrotron energy flux, νF_ν , peaks at $\max[\nu_c, \nu_m]$ (Sari et al. 1998).

Assuming one-shot acceleration, $t_a = t_p$. The synchrotron frequency for the typical energy electrons is larger than the cooling frequency whenever:

$$\gamma_m > 0.46k(k+1)^{-3}\Gamma_{2.5}^5 E_{tot,52.5}^{-1} t_{p,-0.3}^2, \quad (9)$$

where we use the notation: $q_x = q/10^x$ in c.g.s. units here and elsewhere in the text. Fig. 1 depicts the regions in the parameter space where the electrons are slow cooling. We note that for larger radii (larger values of k) the fast cooling regime becomes larger. At large radii both the magnetic field and γ_m are smaller and the cooling is less efficient. For $\Gamma = 50, 300$ the synchrotron is in the fast cooling regime independent of γ_m , R and ϵ_e . For $\Gamma = 1000$ the synchrotron radiating electrons will be fast cooling, unless: $\gamma_m \lesssim 190k(k+1)^{-3} E_{tot,52.5}^{-1} t_{p,-0.3}^2$ (or equivalently $R_{15} \gtrsim 10^2 \gamma_{m,3.5}^{1/2} E_{tot,52.5}^{1/2} t_{p,-0.3}^{-1}$ cm). Thus, by virtue of the strong magnetic fields of the Poynting flux dominated jet, quite generally $\nu_c \ll \nu_m$. This implies a very short cooling time by synchrotron, as: $t_{c,syn}/t_p = (\nu_c/\nu_m)^{1/2}$ (where $t_{c,syn}$ is the cooling time for the typical electron, see Beniamini & Piran (2013) for details).

The synchrotron cooling time and the typical frequency may be affected by self absorption. If self absorption takes place ($\nu_{SSA} > \nu_m$, where ν_{SSA} is the frequency below which synchrotron photons are self absorbed), the synchrotron spectra peaks at ν_{SSA} . In this case, the total luminosity radiated by synchrotron is reduced and the typical cooling time increases by the ratio of the unabsorbed to absorbed synchrotron luminosities. By equating the flux expected from synchrotron to that of a black body with a temperature $kT \approx \gamma_m c^2$, one finds that the synchrotron self absorption frequency will be:

$$\begin{cases} \nu_{SSA} = 10^{14} E_{tot,52.5}^{3/10} \Gamma_{2.5}^{2/5} \gamma_{m,3.5}^{-4/5} R_{15}^{-3/5} t_{p,-0.3}^{-3/10} \text{Hz}, & \nu_m < \nu_{SSA} \\ \nu_{SSA} = 10^{15} A_P E_{tot,52.5}^{\frac{2+p}{10}} \Gamma_{2.5}^{2/5} \gamma_{m,3.5}^{\frac{2p-6}{5}} R_{15}^{-\frac{2+p}{5}} t_{p,-0.3}^{-\frac{2+p}{10}} \text{Hz}, & \nu_{SSA} < \nu_m \end{cases} \quad (10)$$

Where A_p is a numerical function of p which is of order unity for $p \sim 2.5$ and γ_m is taken to be of order 3000 which is its value in case synchrotron radiation is the mechanism producing the sub-MeV peak (Beniamini & Piran 2013). For sufficiently low values of γ_m it is possible that because of self absorption the synchrotron cooling time will increase, but even with this modification the cooling time will be much shorter than the dynamical one.

We plot the cooling time by synchrotron and the peak frequency of the synchrotron signature in Fig. 2 for the ‘‘canonical’’ case of $\Gamma = 300$. The peak synchrotron frequency is either ν_m (for

$\Gamma = 300$ the synchrotron is always “fast cooling”) or ν_{SSA} in cases where the synchrotron becomes self absorbed. We find that the synchrotron can peak anywhere between EUV and HE gamma rays, and has a cooling time shorter than $\sim 10^{-1}$ sec. The short synchrotron cooling time implies that synchrotron is very efficient and the electrons will radiate all their energy within a time scale much shorter than a dynamical time ². Any emission mechanism competing with synchrotron must be even faster in order to tap the electrons’ energy before they are cooled by synchrotron. Even if this mechanism is more efficient than synchrotron (i.e. has a shorter cooling time), the accompanying synchrotron signal may still overproduce optical and X-ray fluxes compared with observations. We consider this possibility in the following sections and find limits on the cooling time associated with any emission process producing the prompt sub-MeV emission in order to sufficiently quench the unobserved synchrotron signature. If synchrotron is responsible for the sub-MeV emission, as can be expected in a magnetic dominated outflow, the electrons must be re-accelerated before cooling to suppress this low-energy emission. In this case these limits set the re-accelerating time needed.

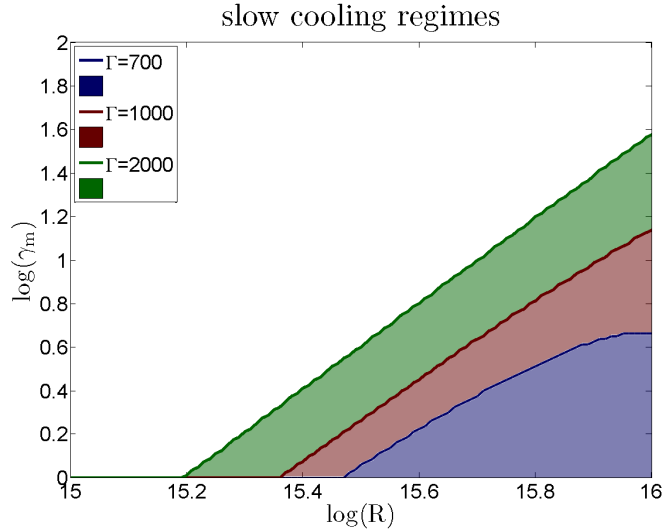


Fig. 1.— Within the colored areas the electrons are slow cooling. Blue, Red and Green correspond to $\Gamma = 700, 1000, 2000$ accordingly. (For values of $\Gamma \lesssim 600$, the synchrotron emitting electrons are always fast cooling). Unless the bulk Lorentz factor is very high, the electrons are most likely fast cooling.

²The fact that the synchrotron cooling timescale is very short was already mentioned almost 20 years ago by Sari & Piran (1995), though in a somewhat different context.

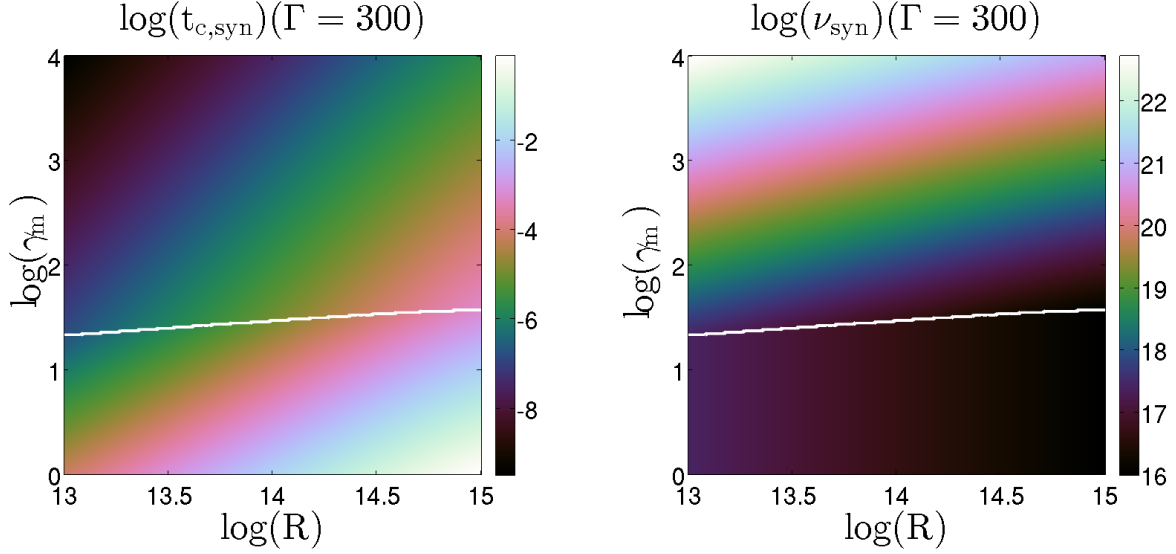


Fig. 2.— Cooling time by synchrotron (left panel) and the synchrotron peak frequency (right panel). The peak frequency is either ν_m (above the white line) or ν_{SSA} (below the line) in cases where the synchrotron signal becomes self absorbed (corresponding to the lower part of the figure). In the self absorbed regime, the frequency depends slightly on ϵ_e . However, in the interest of clarity, we neglect this dependence in these plots and assume a constant $\epsilon_e = 0.1$ in the entire parameter region. The synchrotron can peak anywhere between EUV and HE gamma-rays and cools very rapidly.

4. General Constraints - limits on the parameter space

We turn now to consider different parameter phase space. Some of those constraints are generic while others depends on specific details of the model. The non-thermal high energy tail of the spectrum indicates that the source must be (at least marginally) optically thin for scatterings³:

$$\tau = \frac{N_e \sigma_T}{4(k+1)\pi R^2} \lesssim 10. \quad (11)$$

Notice that for a fixed total electrons' energy $N_e \propto \gamma_m^{-1}$. Therefore:

$$\gamma_{m,3.5\epsilon_e,-1}^{-1} R_{15}^{-1} \Gamma_{2.5}^{-3} E_{tot,52.5} t_{p,-0.3}^{-1} < 10^4. \quad (12)$$

³In photospheric models, the radiation is emitted from the photosphere. Even in this case the optical depth at the emission region cannot be larger than 10

If flow is composed of an electron-proton plasma (as opposed to pairs). The energy of the protons should be smaller than the magnetic energy, hence:

$$\frac{\gamma_m m_e p - 1}{\epsilon_e m_p p - 2} > 1, \quad (13)$$

where m_p is the proton mass. As this limit is more model dependent than the previous two, we do not use it as a rigid limit on the parameter space.

SSC is an inevitable byproduct of synchrotron radiation. This emission should also be below the observed limits. A full analysis of SSC can be found in (Nakar et al. 2009; Bošnjak et al. 2009), and a simplified one zone model is described in Beniamini & Piran (2013). Since for magnetically dominated outflows the Compton parameter is small, limits from SSC do not further constrain the parameter space.

The allowed parameter space (for the “canonical” case of $\Gamma = 300$), taking into account the above limits, is shown in Fig. 3. The black area in the figure, is where the synchrotron signal produces the main sub-MeV peak (Beniamini & Piran (2013)).

4.1. Constraints on the parameter space from the observed fluxes

Observations in the optical, X-ray and GeV bands provide further limits on the gamma ray emitting mechanism. They show that t_c (the cooling time associated with the gamma ray emitting mechanism) has to be significantly smaller than the synchrotron cooling time, $t_{c, syn}$ in order not to overproduce synchrotron flux as compared with observations in these bands. Alternatively, the synchrotron emitting electrons must be re-accelerated on this time scale. The synchrotron flux in any band is proportional to the ratio of the cooling time of the (undetermined) prompt emission mechanism to the overall cooling times: $x_t \equiv t_c / t_{c, syn} + t_c \leq 1$. In a given observed band, one requires $t_c / t_{c, syn} < F_{\nu_{obs, A}} / F_{\nu_{syn, A}}$ where $F_{\nu_{syn, A}}$ is the synchrotron spectral flux and $F_{\nu_{obs, A}}$ is the observed limit on the spectral flux and A stands for opt, X or GeV.

4.1.1. Optical limits

Prompt optical fluxes (in the V band) span almost five orders of magnitude in flux, from $100\mu\text{Jy}$ to 3Jy ($7.5 < V < 19$) while contemporaneous gamma ray detections span from $6\mu\text{Jy}$ to 4mJy (Yost et. al. 2007). find that for individual bursts, the ratio $F_{\nu_{obs, \gamma}} / F_{\nu_{obs, opt}}$, of gamma-ray to optical flux is somewhat less variable, and spans from: $2 \times 10^{-3} - 1$. Using TAROT observations in the optical (R) band, Klotz (2009) estimated that $5 - 20\%$ of GRBs have prompt optical emission at the level of $\sim 10\text{mJy}$ ($R < 14$) while more than 50% of bursts have prompt optical fainter than 2mJy ($R = 15.5$). As a typical limit, we take here $F_{\nu_{obs, opt}} = 1\text{mJy}$ at the V-band.

To estimate the synchrotron flux we recall that there are three relevant orderings of the synchrotron frequencies ν_{SSA} , ν_a , and ν_m which cover the majority of cases considered here. Consider first, $\nu_c < \nu_{SSA} < \nu_{opt} < \nu_m$ which happens whenever:

$$\gamma_{m,3.5} > 0.15k^{1/8}(k+1)^{5/8}\epsilon_{e,-1}^{1/2}\Gamma_{2.5}^{-1}E_{tot,52.5}^{3/8}t_{p,-0.3}^{-9/8}\nu_{opt,14.7}^{-5/4}x_t^{1/2}, \quad (14)$$

where $\nu_{opt,14.7}$ is the average v-band frequency. In this case, the synchrotron optical flux is not self absorbed: $F_{\nu_{syn,opt}} = F_{\nu_m}(\nu_m/\nu_{opt})^{1/2}$. As a result, the limit from observations in the optical band becomes highly constraining in this regime:

$$\gamma_{m,3.5} > 10^3\epsilon_{e,-1}\Gamma_{2.5}k^{1/4}(k+1)^{-3/4}E_{tot,52.5}^{3/4}t_{p,-0.3}^{-1/4}\nu_{opt,14.7}^{-1/2}F_{\nu_{opt,1mJy}}^{-1}x_t, \quad (15)$$

where $F_{\nu_{opt,1mJy}} \equiv F_{\nu_{obs,opt}}/1mJy$, $\epsilon_{e,-1} = \epsilon_e/0.1$. Since $F_{\nu_{syn,opt}} \propto \gamma_m^{-1}$, γ_m has to be large in order for the synchrotron to peak at energies much beyond the optical band and the optical synchrotron flux will be sufficiently low. In order to satisfy this limit the cooling time of the gamma ray emitting mechanism should be significantly shorter compared with the synchrotron cooling time i.e. a low value of x_t .

For intermediate values of γ_m :

$$0.03k^{\frac{3}{14}}(k+1)^{\frac{-5}{14}}\epsilon_{e,-1}^{\frac{1}{7}}\Gamma_{2.5}^{\frac{3}{7}}E_{tot,52.5}^{\frac{-1}{7}}t_{p,-0.3}^{\frac{3}{14}}x_t^{\frac{1}{7}} < \gamma_{m,3.5} < 0.15k^{\frac{1}{8}}(k+1)^{\frac{5}{8}}\epsilon_{e,-1}^{\frac{1}{2}}\Gamma_{2.5}^{-1}E_{tot,52.5}^{\frac{3}{8}}t_{p,-0.3}^{-\frac{9}{8}}\nu_{opt,14.7}^{\frac{-5}{4}}x_t^{\frac{1}{2}}, \quad (16)$$

the optical spectrum is suppressed due to self-absorption (i.e. $\nu_{opt} < \nu_{SSA}$). In the thermal part of the spectrum, the flux scales as $F_\nu \propto R^2T$ (where $T \propto \gamma_m$ is the temperature of the electrons). Thus, for sufficiently low values of γ_m , the temperature and hence optical flux will be below the observed limit, independently of the total energy of the outflow, E_{tot} . The corresponding limit on γ_m and R is:

$$R_{15}^2\gamma_{m,3.5} < 3 \times 10^{-5}\Gamma_{2.5}\nu_{opt,14.7}^{-2}F_{\nu_{opt,1mJy}}x_t^{-1}. \quad (17)$$

It is relevant only for small values of R .

Finally, for:

$$\gamma_{m,3.5} < 0.03k^{3/14}(k+1)^{-5/14}\epsilon_{e,-1}^{1/7}\Gamma_{2.5}^{3/7}E_{tot,52.5}^{-1/7}t_{p,-0.3}^{3/14}x_t^{1/7}, \quad (18)$$

the typical synchrotron frequency, ν_m , drops below the self absorption frequency. Here, the order of frequencies is $\nu_c < \nu_{opt}, \nu_m < \nu_{SSA}$. As discussed above, this does not change the limits on the optical flux, which are given directly by the radius of emission and temperature of the electrons. Nonetheless, as the synchrotron peak is self absorbed, the total energy released by synchrotron is reduced in this case, and this causes an increase in the synchrotron cooling time compared with the non-absorbed case (as seen below the white line in Fig. 2).

Fig. 4 depicts $F_{\nu_{syn,opt}}/F_{\nu_{obs,opt}}$ on top of the filled regions which signify the three orderings of frequencies that were discussed above. Large R and γ_m lead to $F_{\nu_{syn,opt}}/F_{\nu_{obs,opt}} \gg 1$ and subsequently yield strong upper limits on the required cooling time of the gamma ray emission mechanism.

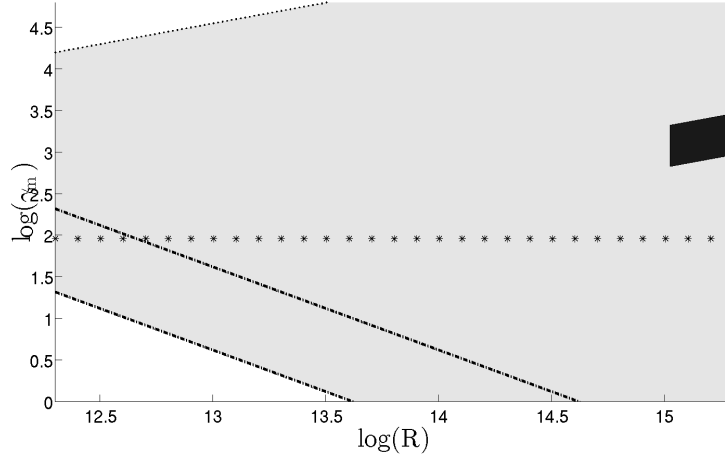


Fig. 3.— The allowed region in the parameter phase space (gray region) in a magnetically dominated jet with $\Gamma = 300$. The conditions $\tau < 1, 10$ (dot-dashed lines) and $\gamma_m < \gamma_{max}$ (dotted line) define general limits on the parameter space. If the flow is composed of a proton-electron plasma, the energy of the protons must be smaller than the magnetic energy (that is assumed to dominate). This condition rules out the area below the asterisks for such jets. The black filled region is where synchrotron emission produces the main prompt sub-MeV peak.

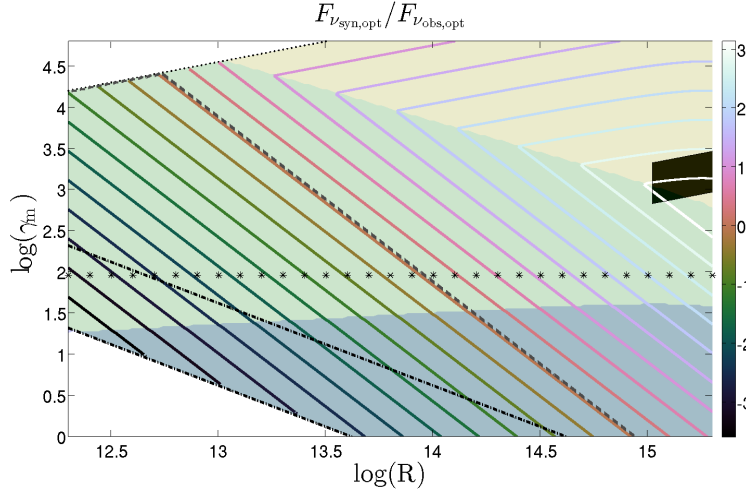


Fig. 4.— Same setup as in Fig. 3. The background colors in these regimes, signify the various possible orderings of frequencies. From top to bottom these are: $\nu_m, \nu_x > \nu_{opt} > \nu_{SSA} > \nu_c$ (no self absorption at the optical band; yellow area), $\nu_m, \nu_x > \nu_{SSA} > \nu_{opt} > \nu_c$ (self absorption at the optical band but not at the peak; green area) and $\nu_x > \nu_{SSA} > \nu_m, \nu_{opt}$ (both the peak and the optical band of the synchrotron are self absorbed; blue area). The ratio of synchrotron optical flux to the observed optical flux is depicted by contour lines. To the right of the gray dashed line, this ratio is larger than one. In this region, the gamma ray process should cool considerably faster than synchrotron in order to reduce the synchrotron flux below the observed limit.

4.1.2. X-ray limits

In some GRBs XRT, the X-ray telescope on board the Swift satellite, observed the bursts during the prompt phase (either in cases where there was a precursor to the main burst or when the burst was very long). From these bursts one can obtain limits on the prompt X-ray flux of GRBs. These turn out to be of the order of 0.5-10mJy ($5 \times 10^{-27} - 10^{-25} \text{erg sec}^{-1} \text{Hz}^{-1} \text{cm}^{-2}$) (Burrows 2005; Campana et al. 2006; Krimm et al. 2006; Moretti et al. 2006; Page et al. 2006; Godet et al. 2007) at the median energy of XRT, which is $\sim 2 \text{keV}$. In all these cases the prompt X-ray lightcurve was seen to track the gamma-rays. Here we pick a canonical limit of $F_{\nu_{\text{obs}, X\text{-rays}}} = 1 \text{mJy}$ at 2keV .

By virtue of Eq. 10 the X-ray band will not be self-absorbed. Therefore, there are two relevant orderings of the frequencies with regard to the X-ray band. If $\nu_m > \nu_x$, the X-ray band falls in the low energy part of the synchrotron spectrum. In this case, as γ_m increases, the synchrotron peak frequency is shifted to higher energies, until it is eventually so high, that the extrapolation of the flux to the X-ray band is below the observed limits. In essence, this is the same kind of limit as given by Eq.15 but now it is applied to the X-ray instead of to the optical band. If $\nu_m < \nu_x$, the X-ray band falls in the high energy part of the synchrotron spectrum. In this case, as γ_m decreases, the synchrotron peak frequency decreases and the synchrotron flux in the X-ray band decreases as well. These two cases can be written as:

$$\begin{cases} \gamma_{m,3.5} > 40 \epsilon_{e,-1} \Gamma_{2.5} k^{1/4} (k+1)^{-3/4} E_{\text{tot},52.5}^{3/4} t_{p,-0.3}^{-1/4} \nu_{X,17.7}^{-1/2} F_{\nu_{X,1\text{mJy}}}^{-1} x_t \text{cm}, & \nu_x < \nu_m \\ \gamma_{m,3.5} < 8 \times 10^{-4} \epsilon_{e,-1}^{-1} \Gamma_{2.5} k^{1/4} (k+1)^{-3/4} E_{\text{tot},52.5}^{-5/4} t_{p,-0.3}^{7/4} \nu_{X,17.7}^{3/2} F_{\nu_{X,1\text{mJy}}} x_t^{-1} \text{cm}, & \nu_m < \nu_x \end{cases} \quad (19)$$

where $\nu_{X,17.7}$ is the XRT median frequency, and $F_{\nu_{X,1\text{mJy}}} \equiv F_{\nu_{\text{obs}, X\text{-rays}}} / 1 \text{mJy}$. Fig. 5 depicts $F_{\nu_{\text{syn}, X\text{-ray}}} / F_{\nu_{\text{obs}, X\text{-ray}}}$. Unless $x_t \ll 1$, either very high or very low values of γ_m (corresponding to $\nu_m \gg \nu_x$ or vice versa) are required in order not to overproduce X-ray radiation.

4.1.3. GeV limits

Another observational limit arises from observations of $\sim 20 \text{MeV} - 30 \text{GeV}$ photons from GRBs with LAT, the HE telescope on board the Fermi mission. From LAT observations it is found that the fluence in the LAT band during the prompt phase is less than 0.1 of the sub-MeV fluence (Guetta et al. 2011; Beniamini et al. 2011; Ackermann et al. 2012). Most bursts are consistent with an extrapolation of the sub-MeV flux. However, about a 1/3 of the bursts have smaller fluxes at these high energies than expected by extrapolation of the peak flux. Additionally, bursts with LAT detections show a correlation between GBM (sub-MeV) and LAT fluxes.

These limits correspond to $\nu_{\text{syn}, \text{LAT}} F_{\nu_{\text{syn}, \text{LAT}}} > 10^{-7} \text{erg sec}^{-1} \text{cm}^{-2}$. As γ_m increases, the synchrotron peak frequency increases and the fraction of the flux that falls within the LAT band

increases. Therefore this corresponds to an upper limit on γ_m (see Fig. 6):

$$\gamma_{m,3.5} < 3\epsilon_{e,-1}^{-1}\Gamma_{2.5}k^{1/4}(k+1)^{-3/4}E_{tot,52.5}^{-5/4}t_{p,-0.3}^{7/4}. \quad (20)$$

As the low flux in the LAT band could be due to a cut-off in the synchrotron spectrum (e.g. due to pair creation opacity), this is a somewhat weaker constraint than those given by the optical and X-ray fluxes. These are relevant, of course, only for models where a pair creation cutoff is expected at higher energies.

4.2. Results - Limits on the Electrons' Cooling Time

As shown in Figs. 4, 5, 6, observations in the optical, X-ray and GeV bands provide even stronger limits on the efficiency of the gamma ray emitting mechanism. t_c has to be significantly shorter than the synchrotron cooling time, $t_{c,syn}$ in order not to overproduce synchrotron flux as compared with observations in these bands. The combined limits from the optical, X-ray and GeV on the cooling time are shown in Figs. 7, 8, 9 for $\Gamma = 50, 300, 1000$ respectively. Almost everywhere in the parameter space the gamma-ray emitting process has to be extremely efficient in order to avoid excess synchrotron flux in one of the observed bands. The upper limits on t_c typically lie in the range $10^{-11} - 10^{-2}$ sec. The upper limits on t_c become lower with decreasing radius of emission as well as with increasing ϵ_e and γ_m .

5. Implications for the Synchrotron model

The discussion so far has been general and could be applied to any emission process. It explores the constraints that synchrotron radiation imposes when the outflow is Poynting flux dominated. We turn now to explore the implication of the above results when synchrotron itself is the source of the prompt emission. This is in fact the most obvious situation when a magnetic field dominates the energy density in the emitting region, (Mészáros et al. 1997; Piran 2005). In a previous work (Beniamini & Piran 2013) we have examined the general observational constraints on the synchrotron emission of the prompt sub-MeV radiation, for a general magnetic field. The resulting parameter space found in that work (in the limit of large ϵ_B) is reproduced here in the region of the parameter space marked as black areas in Figs. 4, 5, 6.

Given the constraints on the optical and X-ray bands considered in §4.1, the simple one zone synchrotron model for the prompt gamma rays is ruled out for a Poynting flux dominated flow. With such strong magnetic fields, the electrons overproduce both optical and X-ray emission. This inconsistency is related but not equivalent to the familiar result that the gamma-ray spectrum below the observed sub-MeV peak is, quite often, inconsistent with $N_\nu \propto \nu^{-3/2}$ predicted for fast-cooling

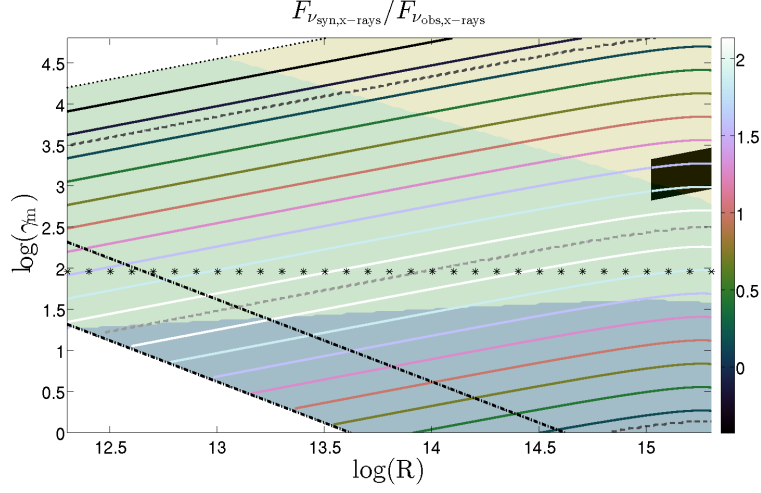


Fig. 5.— Background colors and lines are the same as in Figs. 3,4. The ratio of synchrotron X-ray flux to the observed X-ray flux is depicted by contour lines. Between the dashed gray lines, the ratio is larger than one, requiring the gamma ray process to be more efficient than synchrotron (i.e. have a short cooling time). The lighter dashed gray line in the middle of the figure is $\nu_m = \nu_x$ (below it the X-ray intercepts the high energy part of the synchrotron spectrum and above it the low energy part).

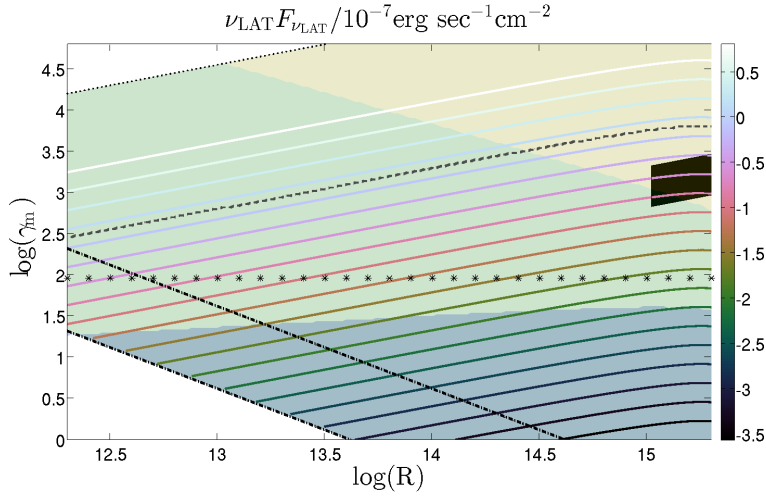


Fig. 6.— Background colors and lines are the same as in Figs. 3,4. The ratio of synchrotron νF_ν in the LAT band to the observed limits in the same band is depicted by contour lines. Above the dashed gray line, the ratio is larger than one, requiring the gamma ray process to be more efficient than synchrotron.

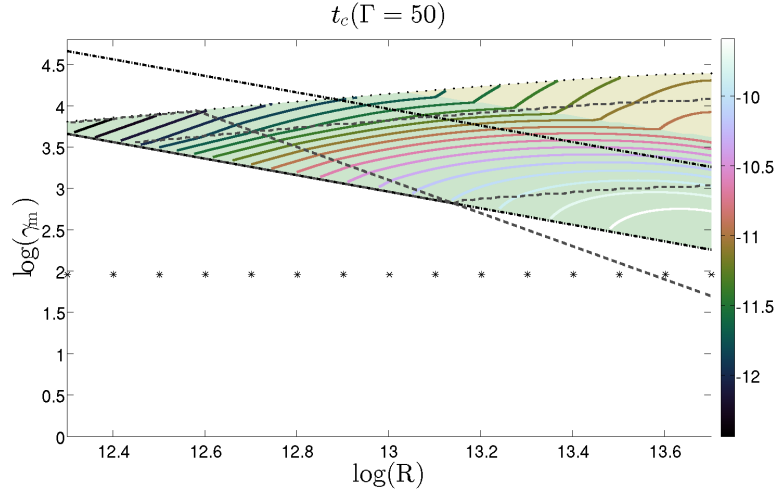


Fig. 7.— Same setup as Figs. 3, 4 for $\Gamma = 50$. In addition, contour lines depict the maximum allowed value for the cooling timescale associated with the gamma-ray producing mechanism (t_c) in order not to overproduce synchrotron emission. t_c should be shorter than $t_{c,syn}$ (the synchrotron cooling timescale) in order for the gamma ray process to be able to tap a significant amount of the electrons' energy. The conditions $F_{\nu_{syn,opt}} < 1 \text{ mJy}$, $F_{\nu_{syn,X-ray}} < 1 \text{ mJy}$ and $\nu_{syn,LAT} F_{\nu_{syn,LAT}} < 10^{-7} \text{ erg sec}^{-1} \text{ cm}^{-2}$ further constrain t_c . Beyond the corresponding lines, t_c should be significantly shorter than $t_{c,syn}$ in order for the synchrotron not to overproduce optical, X-ray or GeV radiation which are unobserved.

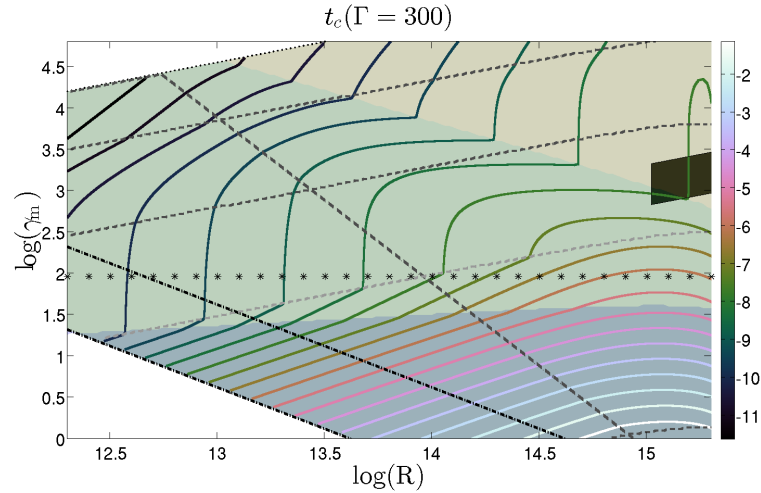


Fig. 8.— Same as in Fig. 7 for $\Gamma = 300$.

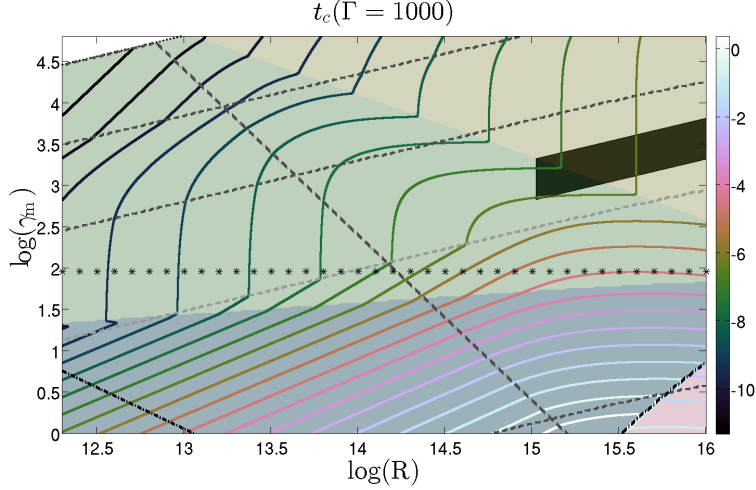


Fig. 9.— Same as in Fig. 7 for $\Gamma = 1000$. The red area at the bottom of the $\Gamma = 1000$ plot (which did not appear previously), signifies where the synchrotron emitting electrons become slow cooling (same as in Fig. 1).

synchrotron (Cohen et al. 1997; Crider et al. 1997; Preece et al. 1998, 2002) and sometimes even with the slow cooling synchrotron, the so called “synchrotron line of death problem”. Clearly, any model that decreases sufficiently fast below the sub-MeV peak will be consistent with the optical and X-ray fluxes, which were obtained assuming that the electrons are fast cooling all the way to the lower energy bands. However, it is possible that refined analysis of the gamma ray spectra will alleviate the problems concerning the gamma-ray spectrum below the sub-MeV peak. For example, recent time resolved spectral analysis (Guiriec 2012) suggests that GRBs are better fitted with a three component model: the Band function, a black body and a power law. Most of the energy is carried out by the Band component. However, the Band component alone is insufficient to fit the entire spectrum. This more complicated fit will change, of course, the relevant low energy spectral index. Given this uncertainty we ignore here this issue of the low energy spectral index and we focus on the optical and X-ray excess problems. As we will see shortly the two models we propose essentially resolve this issue as well.

In order that the synchrotron X-ray flux (at 2keV) will be consistent with the observed limits, the synchrotron cooling frequency must be above the X-ray band. This will lead to a slope (in N_ν) of $\nu^{-2/3}$ up to ν_c followed by the regular (steeper) fast cooling slope of $\nu^{-3/2}$ above ν_c . As a result, the X-ray flux will be lower as compared with the $\nu_c < \nu_x$ case. The condition $F_{\nu_{syn}, X-ray} < F_{\nu_{obs}, X-ray}$, implies:⁴:

$$\left(\frac{\nu_x}{\nu_c}\right)^{1/3} \left(\frac{\nu_c}{\nu_m}\right)^{-1/2} F_{\nu_m} < F_{\nu_{obs}, X-ray} \quad (21)$$

⁴Similar estimates can be applied to the optical band, but these yield weaker constraints on ν_c

or:

$$h\nu_c > (h\nu_m)^{3/5}(h\nu_x)^{2/5} \approx 40\text{keV} \quad (22)$$

where the peak of νF_ν is at ν_m for the fast-cooling synchrotron scenario explored here, and the last equality is for a typical $h\nu_m \sim 300\text{keV}$ (host frame).

Large values of ν_c can be reached in two ways. Either the electrons are re-accelerated before they cool significantly (the “re-acceleration model”) or the electrons escape the radiation zone before cooling down significantly. The latter possibility can be achieved if the magnetic field in the emission zone is highly non homogeneous (the “escape model”). In the following we discuss these two models.

5.1. Re-acceleration

The simplest variant of the re-acceleration model is if the emitting electrons are continuously re-accelerated while emitting (Ghisellini and Celotti 1999; Kumar & McMahon 2008). A second possibility is to abandon the “one zone” approximation. In this case the electrons are accelerated sporadically within “acceleration sites”, while they emit throughout the whole system. Namely, the acceleration sites are immersed in a background “radiation zone” in which the electrons cool down by synchrotron. A critical condition is that a typical electron reaches an acceleration site and is re-accelerated before it cools significantly, thus avoiding excess low energy emission. We keep the nature of the acceleration sites arbitrary, they can be either magnetic reconnection sites, internal shocks or some other plasma instabilities, and discuss some general properties of this model.

Eqs. 22 and 8 imply that, to avoid the low energy emission, the time between accelerations is:

$$t_a \approx 2 \times 10^{-5} \Gamma_{2.5}^4 (k+1)^{-9/4} k^{3/4} E_{tot,52.5}^{-3/4} t_{p,-0.3}^{9/4} \text{ sec.} \quad (23)$$

For canonical parameters, this is $\sim 5 \times 10^4$ shorter than the pulse’s duration. Namely, to avoid excessive cooling each particle has to be accelerated 5×10^4 times during a single pulse. This implies that, compared with the number of electrons needed for the single-shot acceleration, 5×10^4 times fewer electrons are needed to produce the same flux. Assuming an electron-proton plasma and one proton per electron (the later is justified below), this yields a ratio between magnetic and Baryonic flux of:

$$\sigma = 3 \times 10^5 \Gamma_{2.5}^{-3} (k+1)^{3/2} k^{-1/2} E_{tot,52.5}^{1/2} t_{p,-0.3}^{-1/2}. \quad (24)$$

This ratio is extremely large and as such it poses another constraint on the system. This high σ parameter will affect the jet dynamics. Specifically, the reverse external shock associated with such highly magnetized flows is very weak and this could affect the early afterglow signal.

Each acceleration episode has to recreate, (more or less) the initial energy spectrum of the electrons $dN/d\gamma \propto \gamma^{-p}$ for $\gamma_m < \gamma < \gamma_{max}$ with $\gamma_m \gg 1$. Before each acceleration, the

accelerated electrons are at γ_c (where γ_c is the Lorentz factor of an electron radiating synchrotron at ν_c : $\nu_c = \Gamma \gamma_c^2 \frac{q_e B}{2\pi m_e c}$) and a typical electron is accelerated to γ_m . By virtue of Eq. 22, $\nu_m \gtrsim 10\nu_c$, thus $\gamma_m \gtrsim 3\gamma_c$. This means that a typical electron should be accelerated only by a factor of 3 in each re-acceleration episode. This implies immediately that this model must involve two different acceleration processes. First, an initial acceleration process that accelerates most of the electrons to a large Lorentz factor:

$$\gamma_m = 5000 \Gamma_{2.5} (k+1)^{-3/4} k^{1/4} E_{tot,52.5}^{-1/4} t_{p,-0.3}^{3/4}. \quad (25)$$

Then, a re-acceleration process accelerates an already relativistic electron only modestly. Hence the two acceleration process must be very different. A similar situation occurs in the ICMART model (Zhang & Yan 2011). This complication is of course an intrinsic drawback of the model. Furthermore, the first acceleration process must accelerate all electrons without leaving behind any slow ones (as seen for example in PIC simulations by Spitkovsky (2008); Sironi & Spitkovsky (2011)). Otherwise, unless a specific mechanism prevents the re-acceleration sites from accelerating mildly relativistic electrons these electrons will be eventually accelerated and produce spurious emission that will contradict the observations.

Outside the acceleration sites, the electrons emit synchrotron radiation while propagating along the field lines. The propagation time between sites should be at most t_a in order to avoid excess soft radiation. The mean free path between encounters with acceleration sites, λ' , is simply:

$$\lambda' = ct'_a = \Gamma ct_a = 2 \times 10^8 \Gamma_{2.5}^5 (k+1)^{-9/4} k^{3/4} E_{tot,52.5}^{-3/4} t_{p,-0.3}^{3/2} \text{cm} \quad (26)$$

where primes denote quantities in the comoving frame. This determines the number of sites (N_s) in terms of the size of an acceleration site, l' :

$$N_s = \frac{4R^3 k}{\Gamma \lambda' l'^2}. \quad (27)$$

We denote by d' the typical distance between acceleration sites. Using

$$4\pi R^2 \frac{kR}{2\Gamma} \approx N_s \frac{4\pi}{3} \left(\frac{d'}{2}\right)^3, \quad (28)$$

we obtain:

$$d' = \left(\frac{12kR^3}{\Gamma N_s}\right)^{1/3} = (3\lambda' l'^2)^{1/3} \lesssim \lambda'. \quad (29)$$

Eq. 29 can also be written as:

$$\frac{l'}{d'} = \left(\frac{l'}{3\lambda'}\right)^{1/3}. \quad (30)$$

The smallest plausible size for an acceleration site is the Larmor radius of the highest energy electrons one wishes to accelerate. Given that the high energy power law above the peak of the

observed Band function extends up to $\sim 500\nu_p$, there should be electrons with Lorentz factors up to $\gamma \approx 20\gamma_m$. Taking the Larmor radius of these electrons as the minimal size of an acceleration site we obtain:

$$0.03\Gamma_{2.5}^{-1/3} < \frac{l'}{d'} < 1. \quad (31)$$

where the exact value depends on the acceleration mechanism. These results suggest that while the acceleration sites could be small they can also approach the continuous limit. In continuous acceleration, an equilibrium may be reached between heating and cooling such that electrons of some specific energy remain at a constant energy, and do not overproduce low energy photons (Kumar & McMahon 2008). In this case, $\nu_c \approx \nu_m$ and the low energy spectral slope problem is resolved as well.

5.2. The escape model

Alternatively, the spurious low energy synchrotron emission can be avoided if the electrons escape from the emitting region before they cool down. In this way the effective cooling frequency ν_c will be determined by the escape time of the electrons from the emitting region and not by the hydrodynamic time scale. As the size of the system is of order ct_{hyd} we cannot expect that the electrons will physically leave the region. However, if the system is sufficiently inhomogeneous such that in addition to the high magnetic field region in which the electrons cool rapidly there are regions of low magnetic field in which the electrons are slow cooling, then the electrons can escape the emitting zones before cooling significantly. We discuss here the possible structure of such a configuration.

We consider a model in which there are two typical magnetic fields. A strong field with a (co-moving) magnetic field strength B'_s and a weak field region where the magnetic field is B'_{out} , $\eta_B \equiv B'_s/B'_{out}$. The fields are such that electrons radiate efficiently only while passing through the “radiation sites” in which the magnetic field is strong. As we are considering a Poynting flux dominated system in which the magnetic fields carry most of the energy of the system there are two different regimes. In the first the magnetic field energy in the background dominates the energy of the system while in the second the total energy of the radiation sites dominates.

An electron with a Lorentz factor γ spends a time $t_s(\gamma)$ in the radiation sites. In case the electron only encounters one site during the pulse duration, this is the escape time from a single site. Otherwise, it is the total time it spends within different radiation sites. In order to maintain the given sub-MeV peak flux, emitted by electrons with $\gamma > \gamma_c$, while reducing the synchrotron optical and X-ray fluxes that arise from electrons with $\gamma < \gamma_c$, t_s must satisfy:

$$\begin{cases} t_s(\gamma) < t_{c,s}(\gamma), & \gamma < \gamma_m/3 \\ t_s(\gamma) > t_{c,s}(\gamma), & \gamma > \gamma_m \end{cases} \quad (32)$$

where $t_{c,s}$ is the synchrotron cooling time in the radiation sites. Since $t_c(\gamma) \propto \gamma^{-1}$, the escape mechanism must satisfy $t_s(\gamma) \propto \gamma^a$ with $a \geq -1$ (the case of $a = -1$ is considered in detail below). We define γ_{esc} as the Lorentz factor of electrons for which $t_s(\gamma) = t_{c,s}(\gamma)$. For $a \geq -1$, electrons with $\gamma > \gamma_{esc}$, will cool before escaping, whereas electrons with $\gamma < \gamma_{esc}$, will escape the emission site before contributing to the low energy flux. For $\gamma_{esc} < \gamma_m$ the spectrum below $\nu(\gamma_{esc})$ will be a regular slow cooling spectrum of $\nu^{-2/3}$. Between $\nu(\gamma_{esc})$ and $\nu(\gamma_m)$ the spectrum will be fast cooling: $\nu^{-3/2}$.

If the escape is dominated by Bohm diffusion, then $t_s(\gamma) \propto \gamma^{-1}$, which is the marginal value of a . In this case the ratio of the escape time to the cooling time is the same for all electron energies. However, as all electrons are assumed to have initially been accelerated to above γ_m , electrons radiate first at $\nu \geq \nu_m$ and only later at lower frequencies. This means that for the marginal value of a , if $t_s(\gamma) \approx t_{c,s}(\gamma)$ (for $a = 1$ if this ever equality holds, it does so for any value of γ), then there would be a reduction of the low energy flux but not of the flux above ν_m as required by observations. If $t_s(\gamma) > t_{c,s}(\gamma)$ the electrons don't escape and one gets the initial (non-escaping spectrum). If $t_s(\gamma) \ll t_{c,s}(\gamma)$ the electrons cool down significantly and over produce optical and x-ray before escaping.

Consider first the situation in which the energy is dominated by magnetic energy of the background field. In this case the total magnetic energy determines B'_s . Using $\nu_m \propto B'_s$ and $B'_s = B'_{out}\eta_B$ we obtain:

$$\gamma_m = 5000\Gamma_{2.5}(k+1)^{-3/4}k^{1/4}E_{tot,52.5}^{-1/4}t_{p,-0.3}^{3/4}\eta_B^{-1/2} \quad (33)$$

$$t_{c,s}(\gamma_m) = 2 \times 10^{-5}\Gamma_{2.5}^4(k+1)^{-9/4}k^{3/4}E_{tot,52.5}^{-3/4}t_{p,-0.3}^{9/4}\eta_B^{-3/2}\text{sec}. \quad (34)$$

To avoid significant cooling of the electrons outside the emission sites, the electrons' energy losses outside these sites should be small compared to the energy loss within the sites:

$$\frac{P_{out}t'_p}{P_s t'_s} = \frac{B'^2_{out}t'_p}{B'^2_s t'_s} = \eta_B^{-2} \frac{t_p}{t_s} < 1, \quad (35)$$

where $P \propto B^2$ is the synchrotron radiated power. Using $t_s \approx t_{c,s}(\gamma_m)$ (from Eq. 32) yields:

$$\frac{P_{out}t'_p}{P_s t'_s} \sim 5 \times 10^4 \eta_B^{-1/2} < 1 \rightarrow \eta_B \gtrsim 2 \times 10^9 \Gamma_{2.5}^{-8} (k+1)^{9/2} k^{-3/2} E_{tot,52.5}^{3/2} t_{p,-0.3}^{-5/2}. \quad (36)$$

Therefore the magnetic field in the sites must be huge compared to the background field. In order for this configuration to be stable over a dynamical time of the system, the magnetic energy density in the sites (η_B^2) must be compensated by a comparable particle pressure in the background. The energy in the background (which in this case, is also the total energy) will be dominated by the particles and not the magnetic fields, contrary to our assumptions.

We turn now to the case where the magnetic energy of the radiation sites dominates. In this case, it is useful to express the various quantities in the radiation sites in terms of the same quantities in the single-zone model. First, by requiring that the magnetic energy is dominated by the sites, we get:

$$\eta_B^2 x_V > 1, \quad (37)$$

where x_V is the fraction of the volume occupied by the radiation sites. Comparing with the single-zone case, we get: $B'_s = B'_1 x_V^{1/2}$, where B'_1 is the magnetic field in a single-zone model. Next, setting ν_m at the observed gamma-ray peak, we get: $\gamma_m \propto B_s'^{-1/2}$. Using these expressions we find: $t_{c,s}(\gamma_m) \propto B'^{-2} \gamma_m^{-1} \propto t_{c,1}(\gamma_m) x_V^{-3/4}$ where $t_{c,1}(\gamma_m)$ is the cooling time for electrons with γ_m in a single-zone model.

The condition that the total synchrotron energy emitted in the radiation sites is larger than the energy emitted between sites yields:

$$\frac{B_{out}^2 t'_p}{B_s'^2 t_{c,s}(\gamma_m)'} = \eta_B^{-2} \frac{t'_p}{t'_{c,1}} x_V^{3/4} < 1. \quad (38)$$

Combining Eqs. 38, 37 yields:

$$\eta_B > \left(\frac{t'_p}{t'_{c,1}}\right)^{2/7} = 20 \Gamma_{2.5}^{-8/7} (k+1)^{9/14} k^{-3/14} E_{tot,52.5}^{3/14} t_{p,-0.3}^{-5/14}, \quad (39)$$

$$x_V < \left(\frac{t'_p}{t'_{c,1}}\right)^{-4/7} = 2 \times 10^{-3} \Gamma_{2.5}^{16/7} (k+1)^{-9/7} k^{3/7} E_{tot,52.5}^{-3/7} t_{p,-0.3}^{5/7}. \quad (40)$$

The jump in magnetic energy density is smaller than in the previous case. Still it must be balanced by a pressure in the background. Since the volume of the sites is smaller than that of the background, this would imply that the total particles' energy in the background is larger than the total magnetic energy, which was assumed to be dominant. Note however, that such a model may be relevant for resolving the low energy spectral index problem in a situation where the energy is not dominated by the magnetic field.

6. Conclusions

We have explored the conditions within magnetically dominated emission regions with minimal assumptions on the specific radiation mechanism responsible for the sub-MeV peak, focusing on the synchrotron signature of relativistic electrons that are present there. We find that for $\Gamma \lesssim 600$ relativistic electrons that are accelerated on a time scale shorter than the dynamical time scale, will cool rapidly by synchrotron emission. Therefore, any radiation mechanism proposed to explain the sub-MeV peak that relies on relativistic electrons should be faster than synchrotron. As such a

mechanism is not known, synchrotron is the main emission mechanism in magnetically dominated systems. If synchrotron produces the prompt sub-MeV emission, the electrons cool extremely rapidly. For example, within an outflow with a typical Lorentz factor $\Gamma = 300$, the cooling time associated with the gamma ray emitting process, is at least one order of magnitude shorter than the pulse time scale. The typical cooling frequency will be below the X-rays and in many cases even below optical. This implies that synchrotron emission from these fast cooling electrons will be far above observational limits in the X-ray and in the optical. This problem is related, but not directly similar, to the low energy spectral index of the prompt γ emission which is much harder than the one predicted by fast cooling.

There are two possible ways to overcome the excessive emission at low frequencies. The electrons can be accelerated before they cool down or they can escape rapidly from the large magnetic field zone. The acceleration can be continuous Ghisellini and Celotti (1999); Kumar & McMahon (2008). In this case the electrons are kept more or less at the same Lorentz factor during the whole emission episode. Alternatively the acceleration can be sporadic and the electrons are accelerated within “re-acceleration sites” (this is the situation in e.g. the ICMART model Zhang & Yan (2011)). The acceleration in these “re-acceleration sites” should be modest, by a factor less than three in energy. This implies that this scenario requires two different acceleration process. First an initial acceleration that brings the electrons to $\gamma_m \sim 5000$ and then a second re-acceleration process that accelerates the electrons mildly. An additional constraint is that all electrons present must be accelerated in the first acceleration phase, otherwise slow electrons would be accelerated to mild energies within the “re-acceleration sites” and will produce spurious low-energy synchrotron emission. Due to the re-acceleration only very few electrons are needed to produce the observed flux. Hence, only very few protons must be present in the outflow. Consequently all acceleration models require a very small baryonic loading (an extremely large σ).

An alternative scenario is one in which the magnetic field is inhomogeneous and the electrons cool efficiently only in “emission sites” in which the magnetic field is stronger. However, this model requires that the magnetic field within the emission sites should be significantly larger than the field in the outer regions. This requires an external source of pressure that confines the magnetic field in the emission sites and it is incompatible with the situation which we consider in which the outflow is Poynting flux dominated. This might be applicable, however, in other situation in which the magnetic field is weaker.

To summarize, we find that very specific conditions have to be satisfied if the emitting region is Poynting flux dominated. Any model in which the emission is in such a region must demonstrate how these conditions are reached to be viable. To our knowledge there is no known physical model that indeed demonstrates how these conditions can be met. The simplest possible resolution of this conundrum is that the outflow is not Poynting flux dominated in the emission region. This implies that Poynting flux dominated jets dissipate their magnetic energy before the emission zone. Inter-

estingly very different considerations, based on examination of propagations of relativistic MHD jets within stellar envelope, have led recently Bromberg et al. (2014) to reach a similar conclusion, namely that Poynting flux dominated jets must dissipate deep in the interior of Collapsars in order to be compatible with observations.

We thank Jonathan Granot, Rodolfo Barniol Duran and Daniel Kagan for helpful discussions. This research was supported by the ERC advanced research grant “GRBs”, by the I-CORE (grant No 1829/12) and by ISF-NSFC research grant.

REFERENCES

- Achterberg, A., Y. A. Gallant, J. G. Kirk, and A. W. Guthmann, 2001, *Mon. Not. RAS* 328.
- Ackermann, M., et al., 2012, *ApJ*, 754, 121T.
- Aharonian, F.-A., et al. 2009, *A&A*, 495, 505.
- Albert, J. et al. 2006, *ApJ*, 641, L9.
- Ando, S., Nakar, E. & Sari, R. 2008, *ApJ* 689, 1150.
- Atkins, R. et al. 2005, *ApJ*, 630, 996.
- Axelsson, M., et al. 2012, *ApJ*, 757, L31.
- Barniol Duran, R. & Kumar, P., 2011, *MNRAS* 412, 522.
- Beloborodov, A. M., Sep. 2010. Collisional mechanism for gamma-ray burst emission. *MNRAS* 407, 1033.
- Bednarz, J., and M. Ostrowski, 1998, *Physical Review Letters*, Volume 80, Issue 18, May 4, 1998, pp.3911-3914 80, 3911.
- Beniamini, P., Guetta, D., Nakar, E., Piran., T. 2011, *MNRAS*, 416:3089.
- Beniamini, P. & Piran, T., 2013, *ApJ*, 769, 69B.
- Bošnjak, Ž., Daigne, F., and Dubus, G. *A&A* 498, 677 (2009).
- Bromberg, O., Granot, J., Luybarsky, Y., and Piran, T., in preparation (2014).
- Burrows, D. N. et al. 2005a, *Space Science Reviews*, 120, 165—. 2005b, *Science*, 309, 1833.
- Campana, S. et al. 2006, *GCN circ.*, 5168.

Cohen, E., J. I. Katz, T. Piran, R. Sari, R. D. Preece, and D. L. Band, 1997, *Ap. J.*, 488, 330+.

Crider, A., Liang, E. P., Smith, I. A., Preece, R. D., Briggs, M. S., Pendleton, G. N., Paciesas, W. S., Band, D. L., & Matteson, J. L. 1997, *ApJ*, 479

de Jager, O. C., A. K. Harding, P. F. Michelson, H. I. Nel, P. L. Nolan, P. Sreekumar, and D. J. Thompson, 1996, *Ap. J.*, 457, 253.

Eichler D., Levinson A., 2000, *ApJ*, 529, 146.

Fan, Y. Z. & Piran, T. 2006, *MNRAS*, 369, 197.

Fenimore E. E., Epstein R. I., Ho C., 1993, *A&AS*, 97, 59.

Frail et al. 2000, *ApJ*, 538, L129.

Gallant, Y. A., and A. Achterberg, 1999, *Mon. Not. RAS* 305, L6.

Ghisellini, G., Celotti, A., 1999, *ApJ*, 511, L93.

Giannios D., 2006, *A&A*, 457, 763.

Godet, O., et al. 2007, *GCN circ.*, 6053.

Granot, J., Konigl, A., Piran, T., 2006, *MNRAS*, 370, 1946.

Guetta, D., Pian, E., Waxman, E. 2011, *A&A*, 525, 53.

Guiriec, S., et al. 2011, *ApJL*, 727, L33.

Guiriec, S. et al. 2013, *ApJ*, 770, 32.

Guiriec, S. et al. 2012, *cosp*, 39, 682G.

Kawanaka N., Piran T., Krolik J. H., 2013, *ApJ*, 766, 31

Katz, J. I. 1994, *ApJ*, 432, L107.

Klotz, A., Boër, M., Atteia, J. L., & Gendre, B. 2009, *AJ*, 137, 4100.

Krimm, H. A., et al. 2006, *GCN circ.*, 5311.

Kulkarni et al. 1999, *ApJ*, 522, L97.

Kumar, P. & McMahon, E. 2008, *MNRAS*, 384, 33.

Lithwick Y., Sari R., 2001, *ApJ*, 555, 540.

- Lyutikov, M., & Blandford, R. 2003, ArXiv Astrophysics e-prints: 0312.347.
- Mészáros, P., & M. J. Rees, 1993, Ap. J. Lett., 418, L59+.
- Mészáros, P., & Rees, M. J. 1997b, ApJ, 482, L29.
- Mészáros, P. & Rees, M. J. 2000, ApJ, 530, 292.
- Moretti, A., et al. 2006, GCN circ.,5447.
- Nakar E., Piran T., Sari R., 2005, ApJ, 635, 516.
- Nakar, E., Ando, S., & Sari, R. 2009, ApJ, 703, 675.
- O’Brien, P. T., et al. 2006, ApJ, 647, 1213.
- Page, K. L., et al. 2006, GCN circ.,5823.
- Panaitescu, A., Kumar, P., ApJ, 560, L49.
- Panaitescu, A., & Kumar, P. 2002, 571, 779.
- Peer, A. Mészáros, P. & Rees, M. 2006, ApJ, 642, 995.
- Piran T., 1995, in Bahcall J., Osriker J., eds, Proc., April 1995, preprint (arXiv:9507114).
- Piran, T. 2005, in AIP Conf. Ser. 784, Magnetic Fields in the Universe: From Laboratory and Stars to Primordial Structures, ed. E. M. de Gouveia Dal Pino, G. Lugones, & A. Lazarian (Melville, NY: AIP), 164.
- Piran T., Nakar E., 2010, ApJL, 718, L63.
- Preece, R.D. et al., 1998, ApJL, 506, 23.
- Preece, R.D., et al. 2002, ApJ, 581, 1248.
- Rees, M. J., & Mészáros, P. 1992, MNRAS, 258, 41P.
- Rees, M.J., Mészáros, P., 1994, ApJ, 430, L93.
- Rees, M.-J., & Mészáros, P. 2005, ApJ, 628, 847.
- Roming, P. W. A., et al. 2006, ApJ, 652, 1416.
- Ryde, F. & Peer, A. 2009, ApJ, 702, 1211.
- Sari, R., & Piran, T. 1995, ApJL, 455, L143.

- Sari, R., Narayan, R., & Piran, T. 1996, ApJ, 473, 204.
- Sari, R., and T. Piran, 1997, Mon. Not. RAS 287, 110.
- Sari, R., Piran, T., & Narayan, R. 1998, ApJ, 497, L17.
- Sari R., Piran T., 1999a, ApJ, 517, L109.
- Shemi, A., & Piran, T. 1990, ApJ, 365, L55.
- Sironi, L., Spitkovsky, A., Jan. 2011. Particle Acceleration in Relativistic Magnetized Collisionless Electron-Ion Shocks. ApJ 726, 75.
- Spitkovsky A., 2008, ApJ, 682, L5.
- Thompson, C. 1994, MNRAS, 270, 480.
- Thompson, C., Mészáros, P., & Rees, M. J. 2007, ApJ, 666, 1012.
- Usov, V. V. 1992, Nature, 357, 472.
- Vurm, I., Beloborodov, A.M. & Poutanen, J., 2011, ApJ, 738 ,77.
- Waxman, E., 1997, ApJ, 485, L5+.
- Woods E., Loeb A., 1995, ApJ, 453, 583.
- Yost S. et al, 2007, ApJ, 669, 1107.
- Zhang, B., & Pe'er, A. 2009, ApJ, 700, L65.
- Zhang, B., & Yan, H. 2011, ApJ, 726, 90.
- Zou, Y.-C., & Piran, T. 2010, MNRAS, 402, 1854.